World Journal of Microbiology and Biotechnology (2022) 38:31
https://doi.org/10.1007/s11274-021-03209-w

ORIGINAL PAPER

Development of an optimization pipeline of asymmetric PCR towards the generation of DNA aptamers: a guide for beginners

Tzi Shien Yeoh[1] · Andrew Anna[1,2] · Thean-Hock Tang[1] · Marimuthu Citartan[1]

Received: 5 October 2021 / Accepted: 11 December 2021 / Published online: 6 January 2022

Abstract

Asymmetric PCR is one of the most utilized strategies in ssDNA generation towards DNA aptamer generation due to its low cost, robustness and the low amount of starting template. Despite its advantages, careful optimization of the asymmetric PCR is still warranted to optimize the yield of ssDNA. In this present study, we have developed an extensive optimization pipeline that involves the optimization of symmetric PCR initially followed by the optimization of asymmetric PCR. In the asymmetric PCR, optimization of primer amounts/ratios, PCR cycles, annealing temperatures, template concentrations, Mg^{2+}/dNTP concentrations and the amounts of Taq Polymerase was carried out. To further boost the generation of ssDNA, we have also integrated an additional single-stranded DNA generation method, either via lambda exonuclease or biotin-streptavidin-based separation into the optimization pipeline to further improve the yield of ssDNA generation. We have acquired 700 ± 11.3 and 820 ± 19.2 nM for A-PCR-lambda exonuclease and A-PCR-biotin-streptavidin-based separation, respectively. We urge to develop a separate optimization pipeline of asymmetric PCR for each different randomized ssDNA library before embarking on any SELEX studies.

Graphical abstract

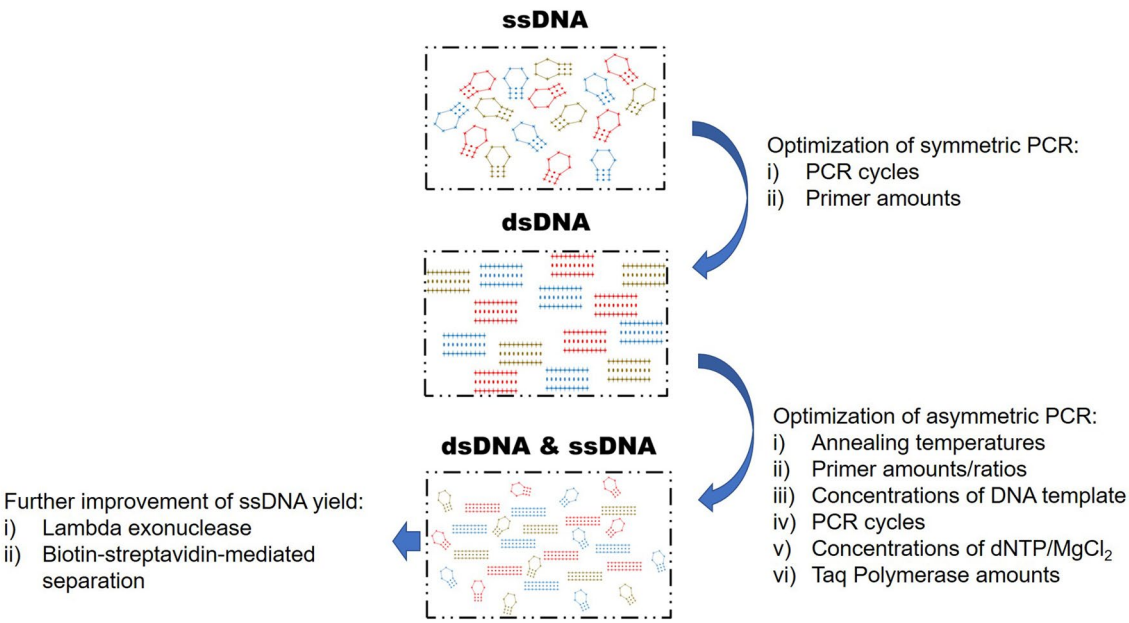

Keywords Asymmetric PCR · Biotin-streptavidin-based separation · Lambda exonuclease digestion · ssDNA

Extended author information available on the last page of the article

Introduction

Having the ability to bind to their targets with high affinity and specificity like antibodies, aptamers are also dubbed as chemical antibodies. Aptamers are single-stranded DNA or RNA that bind to a wide variety of target molecules with high binding affinity and specificity (Tuerk and Gold 1990; Ellington and Szostak 1990). Aptamers fold into a myriad of three-dimensional (3D) structures, which are strengthened by hydrogen-bonding, van der Waals forces and electrostatic charges to forge interaction with their cognate targets for the formation of aptamer-target complex (Hermann and Patel 2000; Nomura, et al. 2010; Piganeau and Schroeder 2003). Since their discovery in the early 1990 (Tuerk and Gold 1990; Ellington and Szostak 1990), aptamers have gradually emerged as a promising class of molecular recognition element (MRE) on par with antibodies due to the following features such as lower cost of synthesis, ability to undergo reversible denaturation and renaturation without the loss of binding capability and low-to-no immunogenicity. Apart from that, aptamers are more versatile than antibodies in term of target selectivity as evidenced in a number of aptamers generated against various targets which are small molecules, protein, viruses and even whole cells (McKeague and DeRosa 2012). Moreover, compared to antibodies, versatility of aptamers also permits chemical modifications to be performed at ease for diagnostic and therapeutic applications (Elskens et al. 2020; Odeh, et al. 2019). Due to their advantages, aptamers are widely used in diagnostics (Liu et al. 2021; Citartan 2021), capturing assays (Citartan et al. 2016), decontamination processes (Bilibana et al. 2017), drug delivery (Thevendran et al. 2020; Citartan 2019), therapeutics (Li et al. 2021) and in vivo imaging (Wang et al. 2021). Aptamers are generated through a process called Systemic Evolution of Ligands via Exponential Enrichment (SELEX). Generally, SELEX is made up of four major steps, which are incubation of the randomized single-stranded DNA/ RNA (ssDNA or RNA) library with the target, partitioning and recovery of the target-bound nucleic acids, amplification of the target-bound nucleic acid molecules via Polymerase Chain Reaction (PCR) for DNA SELEX or Reverse-Transcription Polymerase Chain Reaction (RT-PCR) for RNA SELEX and lastly the regeneration of ssDNA/ RNA for the subsequent round of selection process.

DNA aptamers are preferred over RNA aptamers due to their stability. As DNA SELEX requires the generation of ssDNA, conversion of double-stranded DNA (dsDNA) to ssDNA is of utmost importance in determining the success of an in vitro selection process. Numerous techniques have been introduced (Hao et al. 2020); biotin-streptavidin-based separation (Mosing et al. 2009), lambda exonuclease digestion (Avci-Adali et al. 2009; Citartan et al. 2011), hexaethylene glycol-mediated separation on denaturing urea polyacrylamide gel electrophoresis and asymmetric PCR (A-PCR) (Citartan et al. 2012; Tabarzad, et al. 2014). A-PCR is largely favoured due to its low cost, robustness and the ability to produce a high amount of ssDNA from a minimal input of dsDNA template. By using primers at skewed ratios, ssDNA is anticipated alongside dsDNA by virtue of logarithmic amplification followed by linear amplification. As a starting step prior to any SELEX experiment, optimization of an A-PCR is vital to ensure an optimal production of ssDNA for the subsequent cycles of SELEX, as demonstrated by several previous studies. Tabarzad et al. (2014) have carried out optimization studies involving different annealing temperatures, number of amplification cycles, primer ratios and Mg^{2+} concentrations to find out the optimum parameters (Tabarzad, et al. 2014). Our group have also optimized annealing temperatures and PCR cycles in order to maximize the yield of ssDNA of A-PCR reaction. Another study was carried out by Heiat et al. (2017), whereby the group have optimized primer amounts, ratios, template concentrations, annealing temperatures and PCR cycles (Heiat et al. 2017).

Despite optimization carried out in the previous A-PCR studies, some parameters are often overlooked such as the optimization of the symmetric PCR reactions, the amount of Taq Polymerase and the concentration of Mg^{2+}/dNTP. Impelled by this issue, in the present study, we undertook an effort to develop a much more extensive optimization pipeline that involves the optimization of symmetric PCR. Subsequently, optimization of primer amounts/ratios, PCR cycles, annealing temperatures, template concentrations, Mg^{2+}/dNTP concentrations and the amounts of Taq Polymerase was carried out. We have also integrated an additional single-stranded DNA generation method via lambda exonuclease and biotin-streptavidin-based separation into the optimization pipeline to further improve the yield of ssDNA generation. We propose this optimization pipeline as the first step that can be carried out before initiating any SELEX experiments to augment the yield of ssDNA produced in each SELEX cycle.

Materials and methods

Symmetric PCR amplification

Symmetric PCR amplification was first carried out to prepare the dsDNA template for the A-PCR. A single-stranded DNA library containing randomized region of 40-mer flanked by two fixed primer hybridization regions (5′-ATC

CAGAGTGACGCAGCA-N40-TGGACACGGTGGCTT AGT-3′) was used in this study. The primers used were unmodified forward primer (5′-ATCCAGAGTGACGCA GCA-3′), biotinylated reverse primer (5′-/Biosg/ACT AAG CCA CCG TGT CCA-3′) and phosphorylated reverse primer (5′-/Phos/ACT AAG CCA CCG TGT CCA-3′), which were all purchased from Apical Scientific. All PCR reactions were performed in 100 µL reaction mixture containing 1X PCR buffer [7.5 mM Tris–HCl (pH 9.0), 5 mM KCl and 20 mM $(NH_4)_2SO_4$], 1.5 mM $MgCl_2$, 0.2 mM of dNTPs and 2.5 U DNA Taq polymerase (Biotools). The amount of template used was 20 ng and the PCR parameters were fixed as follow: an initial denaturation at 95 °C for 180 s, followed by amplification cycles of 30 s denaturation at 95 °C, 30 s annealing at 55 °C, 30 s extension at 72 °C and final extension at 72 °C for 300 s. The concentrations of primers were optimized with various amounts of both the forward and reverse primer (10 pmol, 20 pmol, 30 pmol, 40 pmol, 50 pmol, 60 pmol, 70 pmol, 80 pmol, 90 pmol and 100 pmol). The number of amplification cycles were also optimized (1 cycle to 6 cycles). PCR products were run on 4% agarose gel containing 0.5 µL/mL in 1X TAE buffer (40 mM Tris–acetate, 1 mM EDTA) followed by visualization of the PCR products on Gel Doc XR + System (Bio-rad Laboratories). PCR products were subjected to PCR-clean up using Nucleospin Gel & PCR Cleanup (Macherey–Nagel) according to the manufacturer's instructions and dissolved in 25 µL of elution buffer (5 mM Tris–HCl, pH 8.5). Nanodrop spectrophotometer was used to quantify the amount of recovered dsDNA PCR products.

A-PCR

A-PCR reactions were carried out under the similar conditions used in the symmetric PCR except for the different primer ratios of the forward primer to the reverse primer (20:0, 20:0.5, 20:1, 20:2, 50:1 and 100:1). Apart from the primer ratios, different PCR cycles (10 cycles to 30 cycles), different annealing temperatures (55.0 °C, 55.7 °C, 56.9 °C, 58.7 °C, 61.1 °C, 63.0 °C, 64.2 °C and 65.0 °C), different amounts of templates (0.2 ng/µL, 0.4 ng/µL, 0.8 ng/µL and 1.6 ng/µL), different concentrations of $MgCl_2$/dNTP and different amounts of Taq Polymerase (2.5 U, 5.0 U, 10.0 U, 15.0 U, 20.0 U) were also used to determine the optimum parameters. A-PCR products were analyzed using 4% agarose gel electrophoresis and visualized via Gel Doc XR + System.

A-PCR-biotin-streptavidin separation

Following the A-PCR, a scaled-up reaction of up to 1 mL was subjected to biotin-streptavidin separation. First, the A-PCR product was subjected to purification via Nucleospin Gel & PCR Cleanup according to the manufacturer's instructions and dissolved in 100 µL of 0.5X Saline Sodium Citrate buffer, followed by incubation with Streptavidin MagneSphere® Paramagnetic Particles (Promega). Briefly, 400 µL of the bead suspension was aliquoted and transferred to a clean 1.5 mL microcentrifuge tube. A magnet was used to sediment the magnetic particles while the storage buffer was removed. Next, the magnetic beads were then washed thrice with 0.5X Saline Sodium Citrate buffer followed by incubation with the purified A-PCR product at room temperature for 15 min. Following sedimentation of the magnetic beads using magnet, the resulting supernatant was collected. The supernatant was again subjected to Nucleospin Gel & PCR Cleanup and dissolved in 50 µL of ddH_2O. Finally, the amount of ssDNA was quantified using Nanodrop spectrophotometer.

A-PCR-lambda exonuclease digestion

In our second strategy, following the 1 mL-scaled up A-PCR reaction, the resulting product was subjected to lambda exonuclease (Thermo scientific) digestion. Phosphorylated reverse primer was used for the large-scale A-PCR before lambda exonuclease digestion. Upon completion of the A-PCR, the PCR mixtures were purified using Nucleospin Gel & PCR Cleanup. Next, the purified product was dissolved in 44 µL of ddH_2O and subjected to a fifty-microliter lambda exonuclease digestion reaction with the addition of 10 U of enzyme in 1X lambda exonuclease reaction buffer. Digestion time was optimized for 15 min, 30 min, 45 min and 60 min at 37 °C followed by heat inactivation at 80 °C for 10 min. The supernatant was again subjected to Nucleospin Gel & PCR Cleanup and dissolved in 50 µL of ddH_2O. Finally, the amount of ssDNA was quantified using Nanodrop spectrophotometer.

Statistical analysis

The performance of the symmetric PCR was represented by the intensity of the dsDNA band on the agarose gel, which was measured by densitometry analysis with the aid of ImageJ (http://rsb.info.nih.gov/nih-image/). Similarly, the performance of the A-PCR was reflected by the intensity of the band that represents ssDNA, which migrates faster than that of dsDNA. The measured intensity was subjected to Shapiro–Wilk test, to test the nature of the data to assume Gaussian distribution. Following the normality test, the data was subjected to analysis of variance (ANOVA) followed by Tukey's post hoc. All the quantitative results were expressed as mean ± standard deviation. All the experiments were performed in triplicates. T-test and ANOVA were performed using GraphPad Prism 9.0.0, with $P < 0.05$ considered to be statistically significant.

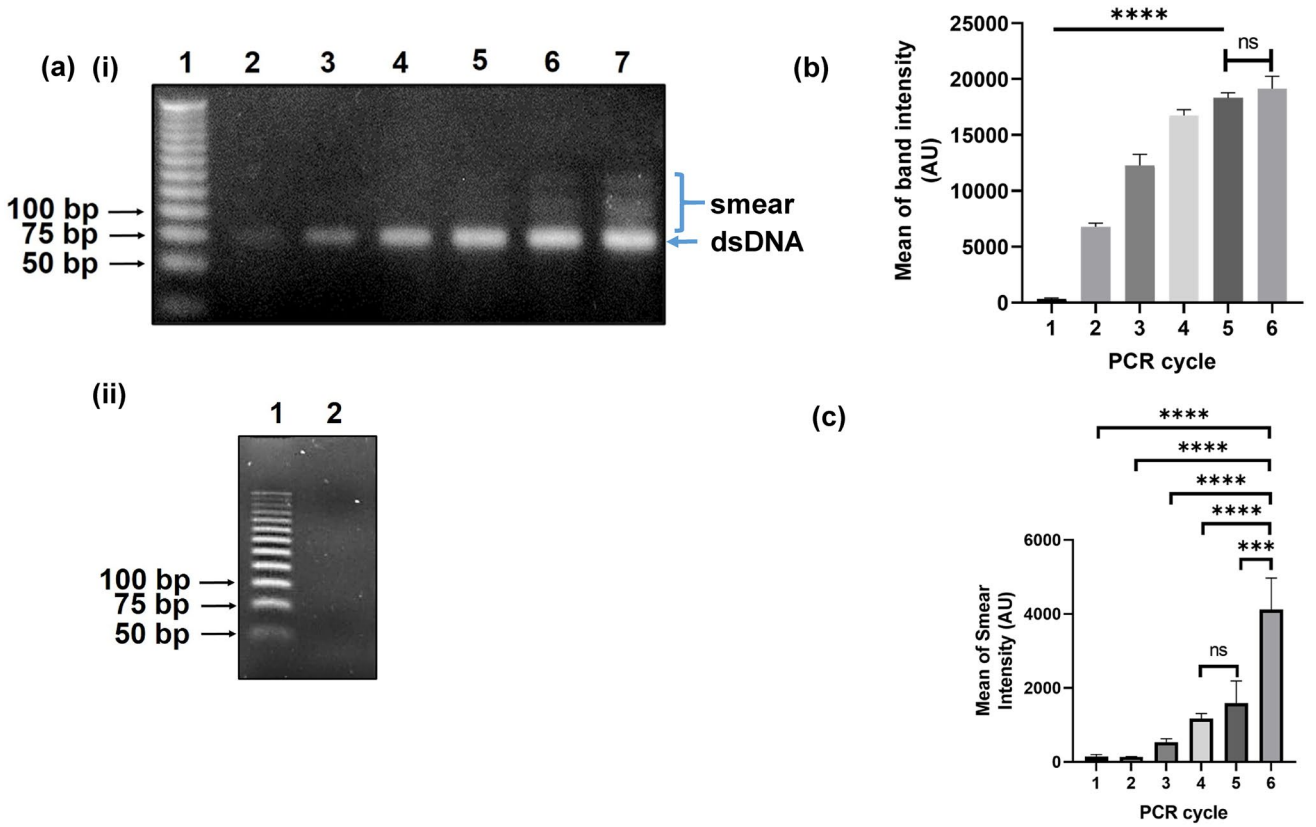

Fig. 1 Effect of number of PCR cycles from 1 to 6 cycles on symmetric PCR amplification. **a** (i) 4% agarose gel electrophoresis of symmetric PCR products produced with different number of PCR cycles. Lane 1: 25 bp DNA ladder, Lane 2: 1 cycle, Lane 3: 2 cycles, Lane 4: 3 cycles, Lane 5: 4 cycles, Lane 6: 5 cycles and Lane 7: 6 cycles. (ii) 4% agarose gel electrophoresis of symmetric PCR product resulting from the usage of 6 PCR cycles in the absence of template. Lane 1: 25 bp DNA ladder, Lane 2: No-Template Control **b** Bar graph of band intensities of dsDNA of symmetric PCR products produced with different number of PCR cycles as estimated by ImageJ analysis. Error bars represent standard deviation of 3 replicates. $P<0.05$ was considered as statistically significant while ****$P<0.0001$ and ns: not significant. **c** Bar graph of band intensities of smear from different number of PCR cycles as estimated by ImageJ analysis. Error bars represent standard deviation of 3 replicates. $P<0.05$ was considered as statistically significant while ***$P<0.001$, ****$P<0.0001$ and ns: not significant

Results

Optimization of symmetric PCR amplification

Prior to the optimization of the A-PCR, symmetric PCR optimization was carried out. First, the effect of the number of PCR cycles on the production of dsDNA was examined. A total of six PCR reactions were prepared and subjected to 1 to 6 PCR cycles. A significant enhancement of the dsDNA band intensity was observed when the number of PCR cycles was increased up to 5 ($P<0.0001$) (Fig. 1a and b). When the PCR cycle was further increased to 6 PCR cycles, there was no significant difference in the dsDNA band intensity between that of cycle 5 and 6. From the smear intensity analysis, the smear intensity stemming from PCR amplification with 6 PCR cycles was significantly higher than that of cycle 5 ($P<0.001$) and the rest of the other PCR cycles ($P<0.0001$) (Fig. 1a and c). However, the smear intensity between the PCR reactions with 4 and 5 PCR cycles showed no significant difference. As such, 5 PCR cycles was selected as the optimum number of PCR cycles due to the much higher dsDNA band intensity than that of 4 PCR cycles ($P<0.0001$).

Next, the optimization that involves the usage of the different amounts of PCR primers from 10 to 100 pmol was carried out. From Fig. 2a and b, it is evident that the production of dsDNA gradually increased with the increasing amount of primers (forward and reverse primers) up to 80 pmol ($P<0.0001$). Further increase in the amount of primers up to 100 pmol resulted in no significant improvement in the production of dsDNA. As such, the primer

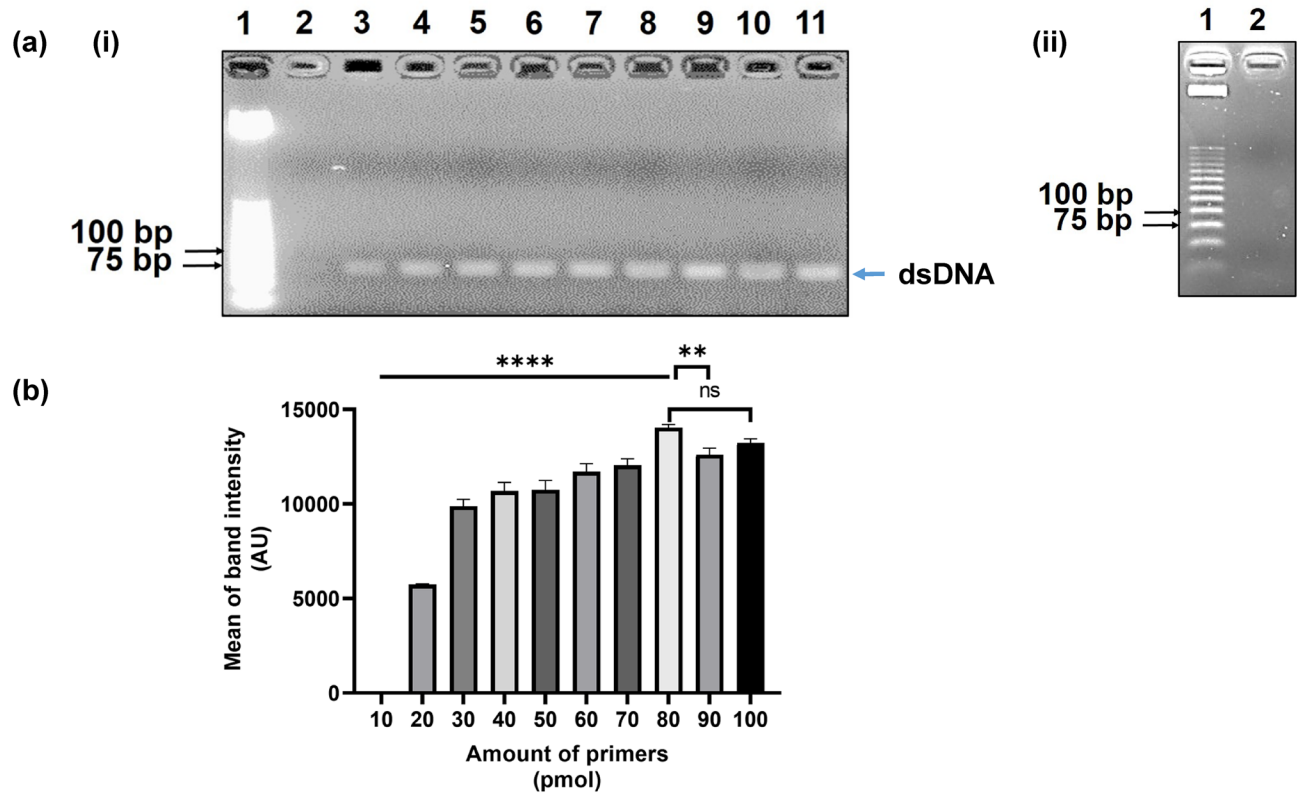

Fig. 2 Effect of amount of PCR primers from 10 to 100 pmol on symmetric PCR amplification. **a** (i) 4% agarose gel electrophoresis of symmetric PCR products produced with different amounts of PCR primers. Lane 1: 25 bp DNA ladder, Lane 2: 10 pmol, Lane 3: 20 pmol, Lane 4: 30 pmol, Lane 5: 40 pmol, Lane 6: 50 pmol, Lane 7: 60 pmol, Lane 8: 70 pmol, Lane 9: 80 pmol, Lane 10: 90 pmol and Lane 11: 100 pmol. (ii) 4% agarose gel electrophoresis of symmetric PCR product resulting from the usage of 100 pmol primer in the absence of template. Lane 1: 25 bp DNA ladder, Lane 2: No-Template Control **b** Bar graph of band intensities of dsDNA of symmetric PCR products produced with different amounts of primers as estimated by ImageJ analysis. Error bars represent standard deviation of 3 replicates. $P < 0.05$ was considered as statistically significant while $^{**}P < 0.01$, $^{****}P < 0.0001$ and ns: not significant

amount chosen was 80 pmol optimum due to the highest production of dsDNA.

The optimization of A-PCR amplification

The purified dsDNA template was subsequently used for the A-PCR reactions. Several different parameters were optimized such as the annealing temperatures, primer ratios, the concentrations of DNA template, the amounts of Taq DNA Polymerase and the concentrations of dNTP/$MgCl_2$.

Annealing temperatures by gradient PCR approach

Out of the 8 different annealing temperatures, the temperature of 56.9 °C was chosen as the best temperature as it resulted in a much higher ssDNA band intensity as compared to that of 55.7 °C ($P < 0.05$), 55.0 °C ($P < 0.01$), 58.7 °C ($P < 0.01$) and the rest of the temperatures (61.1 °C, 63.0 °C, 64.2 °C and 65.0 °C) ($P < 0.0001$) (Fig. 3a and b).

Primer ratios

Different primer ratios were used in the A-PCR amplification, ranging from 20:0, 20:0.5, 20:0.1, 20:2, 50:1 and 100:1. The primer ratio of 50:1 accounted for the highest ssDNA band intensity in the A-PCR reaction ($P < 0.0001$) (Fig. 3c and d). However, the band intensity showed no significant difference as compared to the band intensity resulted when the primer ratio of 100:1 was used for the A-PCR. Thus, the value 50:1 was regarded as the optimum primer ratio for the A-PCR reaction.

Concentrations of DNA template

Using different amounts (0.2 ng/µL, 0.4 ng/µL, 0.8 ng/µL, 1.6 ng/µL) of purified DNA template concentration, the highest concentration that gives the highest band intensity was 1.6 ng/µL ($P < 0.0001$), which was determined as the best template concentration (Fig. 4a and b).

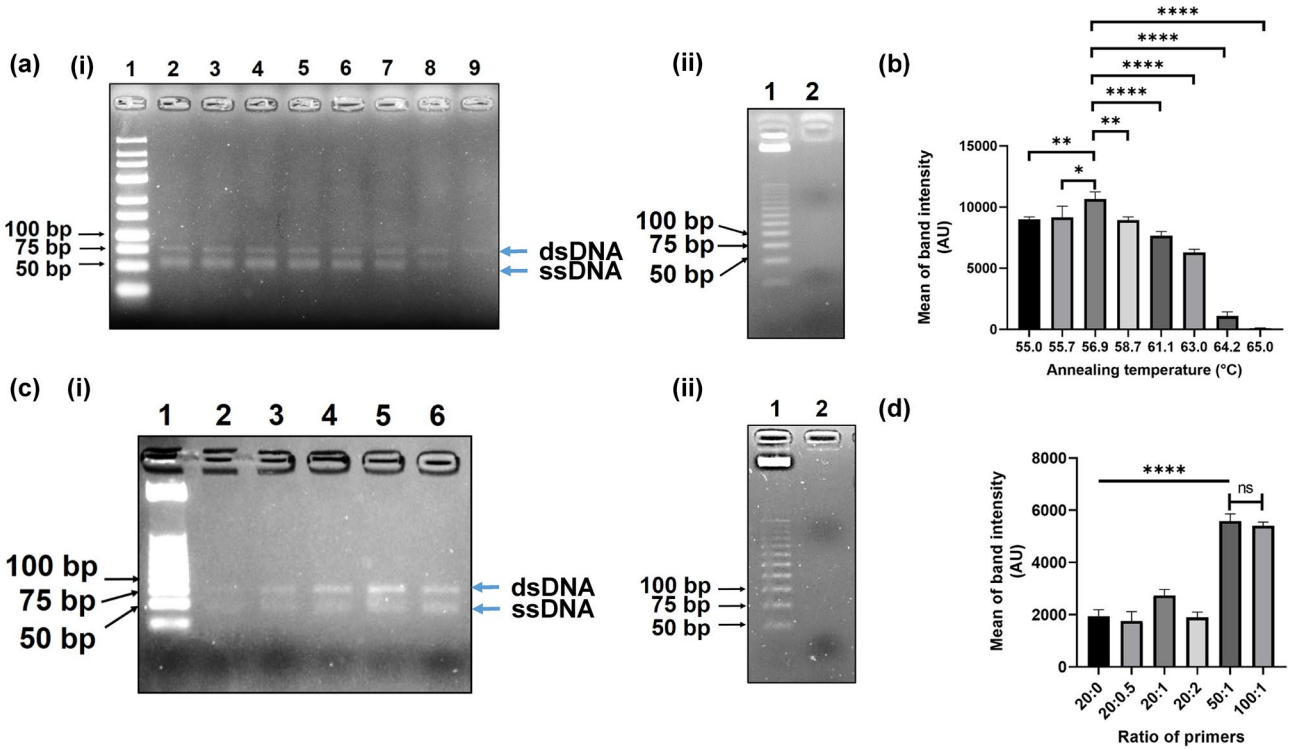

Fig. 3 Effects of annealing temperatures (55.0 °C, 55.7 °C, 56.9 °C, 58.7 °C, 61.1 °C, 63.0 °C, 64.2 °C and 65.0 °C) and primer ratios (20:0, 20:0.5, 20:1, 20:2, 50:1 and 100:1) on A-PCR amplification. **a** (i) 4% agarose gel electrophoresis of A-PCR products produced with different annealing temperatures. Lane 1: 25 bp DNA ladder, Lane 2: 55 °C, Lane 3: 55.7 °C, Lane 4: 56.9 °C, Lane 5: 58.7 °C, Lane 6: 61.1 °C, Lane 7: 63.0 °C, Lane 8: 64.2 °C and Lane 9: 65.0 °C. (ii) 4% agarose gel electrophoresis of A-PCR products resulting from the usage of annealing temperature of 65.0 °C in the absence of template. Lane 1: 25 bp DNA ladder, Lane 2: No-Template Control **b** Bar graph of band intensities of ssDNA (A-PCR) with different annealing temperatures as estimated by ImageJ analysis. Error bars represent standard deviation of 3 replicates. $P < 0.05$ was considered as statistically significant while $*P < 0.05$, $**P < 0.01$ and $****P < 0.0001$. **c** (i) 4% agarose gel electrophoresis of A-PCR products produced with different primer ratios as estimated by ImageJ analysis. Lane 1: 25 bp DNA ladder, Lane 2: 20:0, Lane 3: 20:0.5, Lane 4: 20:1, Lane 5: 20:2, Lane 6: 50:1, Lane 7: 100:1. (ii) 4% agarose gel electrophoresis of A-PCR product resulting from the usage of a primer ratio of 100:1 in the absence of template. Lane 1: 25 bp DNA ladder, Lane 2: No-Template Control **d** Bar graph of band intensities of ssDNA (A-PCR) different primer ratios as estimated by ImageJ analysis. Error bars represent standard deviation of 3 replicates. $P < 0.05$ was considered as statistically significant while $****P < 0.0001$ and ns: not significant

PCR cycles

A-PCR was also optimized in terms of the number of PCR cycles (10, 20 and 30 PCR cycles). From the analysis, it is corroborated that 30 PCR cycles was the optimum number of cycles due to the highest ssDNA band intensity among all ($P < 0.001$) (Fig. 4c and d).

Concentrations of dNTP/$MgCl_2$

Five different final concentrations were used in the A-PCR reaction. The concentrations were 0.2 mM/1.5 mM, 0.4 mM/2.0 mM, 0.6 mM/2.5 mM, 0.8 mM/3.0 mM and 1.0 mM/3.5 mM. There was no significant difference between the ssDNA band intensity of 0.2 mM/1.5 mM and 0.4 mM/2.0 mM concentration of dNTPs/$MgCl_2$-containing A-PCR products. However, increasing the concentrations of dNTPs/$MgCl_2$ up to 0.6 mM/2.5 mM, 0.8 mM/3.0 mM and 1.0 mM/3.5 mM significantly reduces the intensity of the ssDNA band. The lowest concentrations that still produces the highest ssDNA band intensity was finally determined to be 0.2 mM and 1.5 mM, respectively for dNTP and $MgCl_2$ (Fig. 5a and b).

Amounts of Taq DNA Polymerase

Another parameter optimized was the amount of Taq DNA Polymerase. Out of the 5 different units (2.5 U, 5.0 U, 10.0

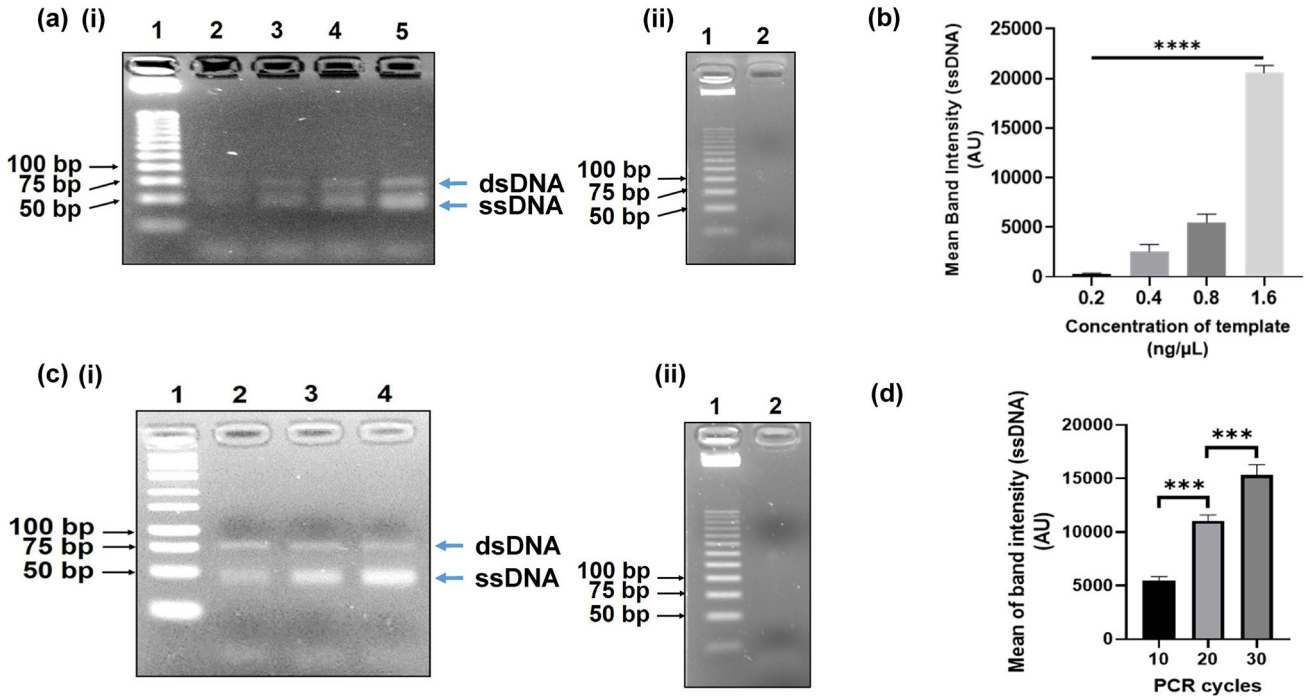

Fig. 4 Effects of the amounts of templates (0.2 ng/µL, 0.4 ng/µL, 0.8 ng/µL and 1.6 ng/µL) and the number of PCR cycles (10 cycles, 20 cycles and 30 cycles) on A-PCR amplification. **a** (i) 4% agarose gel electrophoresis of the A-PCR products produced with different amounts of templates. Lane 1: 25 bp DNA ladder, Lane 2: 0.2 ng/µL, Lane 3: 0.4 ng/µL, Lane 4: 0.8 ng/µL and Lane 5: 1.6 ng/µL. (ii) 4% agarose gel electrophoresis of A-PCR product produced in the absence of template. Lane 1: 25 bp DNA ladder, Lane 2: No-Template Control **b** Bar graph of band intensities of ssDNA (A-PCR) with different amounts of templates as estimated by ImageJ analysis. Error bars represent standard deviation of 3 replicates. $P<0.05$ was considered as statistically significant while ****$P<0.0001$. **c** (i) 4% agarose gel electrophoresis of the A-PCR products produced with different number of PCR cycles. Lane 1: 25 bp DNA ladder, Lane 2: 10 cycles, Lane 3: 20 cycles and Lane 4: 30 cycles. (ii) 4% agarose gel electrophoresis of A-PCR product resulting from the usage of 30 PCR cycles in the absence of template. Lane 1: 25 bp DNA ladder, Lane 2: No-Template Control **d** Bar graph of band intensities of ssDNA (A-PCR) with different number of PCR cycles as estimated by ImageJ analysis. Error bars represent standard deviation of 3 replicates. $P<0.05$ was considered as statistically significant while ***$P<0.001$

U, 15.0 U and 20.0 U), the usage of 2.5 U of Taq DNA Polymerase was able to produce the highest band intensity. No significant difference of band intensity was observed when 5.0 U and 10.0 U of Taq DNA Polymerase were used. However, adding 15.0 U and 20.0 U resulted in significantly lower band intensity ($P<0.01$, $P<0.0001$) than that of 2.5 U of Taq DNA Polymerase. Since the lowest amount of Taq Polymerase that gave the best amplification was 2.5 U, this was taken as the optimum amount for the A-PCR reaction (Fig. 5c and d).

Time course analysis of Lambda Exonuclease digestion

Time course analysis was carried out to optimize the optimal digestion time by lambda exonuclease enzyme. As short as 15 min is enough for complete digestion and there is no significant difference in the band intensity represented by ssDNA if the digestion time was extended up to 30, 45 and 60 min (Fig. 6a and b).

The effect of the incorporation of the ssDNA generation step on the ssDNA intensity

The intensity of the band represented by ssDNA, generated by A-PCR-lambda exonuclease digestion is significantly higher than the band intensity of the ssDNA produced by A-PCR alone ($P<0.0001$) (Fig. 7a). Equivalently, A-PCR-biotin-streptavidin separation resulted in ssDNA with band intensity significantly higher than that of A-PCR per se ($P<0.001$) (Fig. 7b).

The recovery of ssDNA

The ssDNA generated from the A-PCR, A-PCR-biotin-streptavidin-mediated separation and A-PCR-lambda exonuclease-based digestion was subjected to purification. The yields obtained from 1 mL PCR reaction was 450 ± 10.2 nM, 820 ± 19.2 nM and 700 ± 11.3 nM, respectively for A-PCR, A-PCR-biotin-streptavidin-mediated separation and A-PCR-lambda exonuclease-based digestion (Table 1).

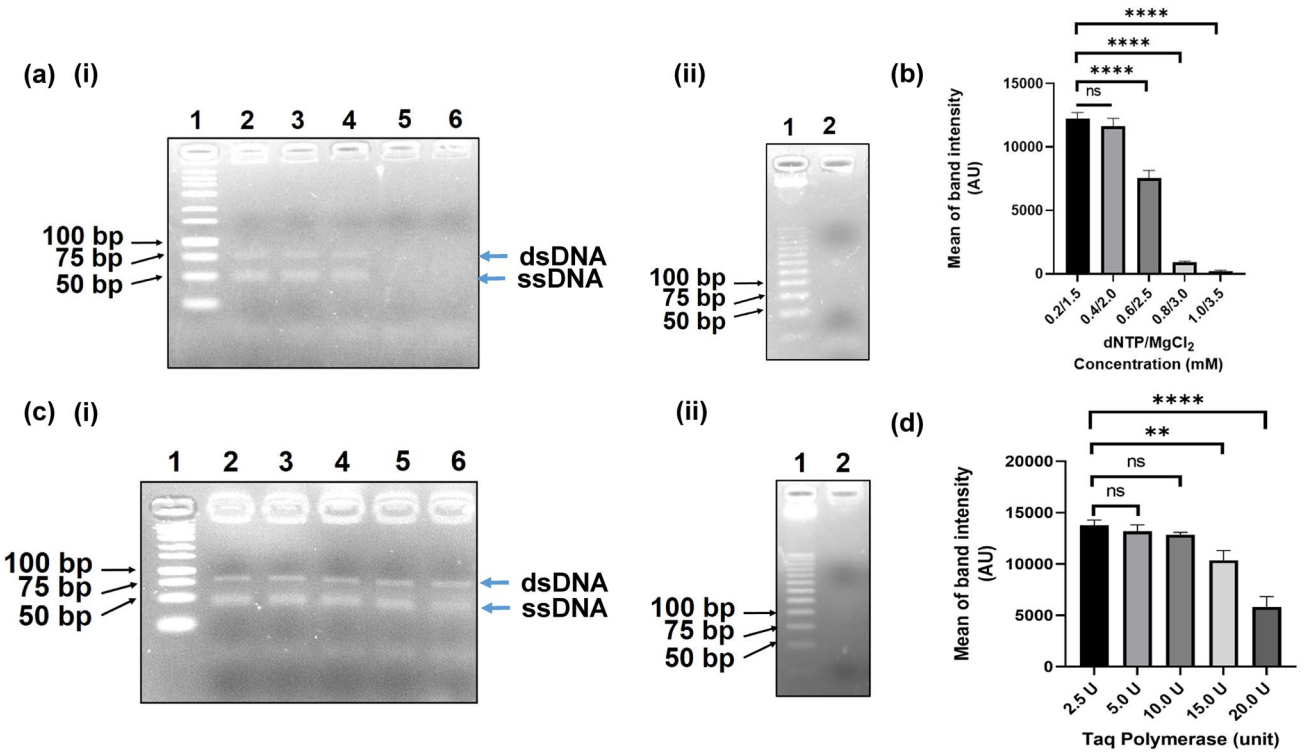

Fig. 5 Effects of dNTPs/$MgCl_2$ (0.2 mM/1.5 mM, 0.4 mM/2.0 mM, 0.6 mM/2.5 mM, 0.8 mM/3.0 mM and 1.0 mM/3.5 mM) and amount of Taq DNA polymerase (2.5 U, 5.0 U, 10.0 U, 15.0 U and 20.0 U) on A-PCR amplification. **a** (i) 4% agarose gel electrophoresis of the A-PCR products produced from different concentrations of dNTPs/$MgCl_2$. Lane 1: 25 bp DNA ladder, Lane 2: 0.2 mM/1.5 mM, Lane 3: 0.4 mM/2.0 mM, Lane 4: 0.6 mM/2.5 mM, Lane 5: 0.8 mM/3.0 mM and Lane 6: 1.0 mM/3.5 mM. (ii) 4% agarose gel electrophoresis of A-PCR product resulting from the usage of 0.2 mM of dNTP/1.5 mM $MgCl_2$ in the absence of template. Lane 1: 25 bp DNA ladder, Lane 2: No-Template Control **b** Bar graph of band intensities of ssDNA (A-PCR) with different concentrations dNTPs/$MgCl_2$ as estimated by ImageJ analysis. Error bars represent standard deviation of 3 replicates. $P<0.05$ was considered as statistically significant while ****$P<0.0001$ and ns: not significant. **c** (i) 4% agarose gel electrophoresis of the A-PCR products produced with different amounts of Taq DNA polymerase. Lane 1: 25 bp DNA ladder, Lane 2: 2.5 U, Lane 3: 5.0 U, Lane 4: 10.0 U, Lane 5: 15.0 U and Lane 6: 20.0 U. (ii) 4% agarose gel electrophoresis of A-PCR product resulting from the usage of 20.0 U of Taq DNA Polymerase in the absence of template. Lane 1: 25 bp DNA ladder, Lane 2: No-Template Control **d** Bar graph of band intensities of ssDNA (A-PCR) with different amounts of Taq DNA polymerase as estimated by ImageJ analysis. Error bars represent standard deviation of 3 replicates. $P<0.05$ was considered as statistically significant while **$P<0.01$, ****$P<0.0001$ and ns: not significant

Discussion

Five PCR cycles and 80 pmol of primers were chosen as the best amplification parameters in the symmetric PCR

DNA SELEX consists of incubation, partitioning, recovery, amplification of bound nucleic acids and generation of ssDNA for the next cycle of SELEX. An optimum symmetric PCR amplification plays a critical role in determining the success of a SELEX experiment, as it is required to amplify the minute amount of the target-eluted sequences to be used in the subsequent cycle of SELEX. An efficient amplification of the symmetric PCR is also instrumental to prepare an optimum dsDNA as the starting template for the A-PCR amplification to ensure a high yield of ssDNA. A-PCR is a two-step procedure, whereby the initial exponential amplification of dsDNA is followed by arithmetic amplification of ssDNA, where transition from the former to the latter phase happens when the limiting primer has been exhausted. In the end of the reaction, ssDNA is produced alongside dsDNA. To expedite the first phase of the A-PCR, template DNA 'feeded' into the reaction must be enough and of high purity to ensure an optimum amplification.

One of the major issues in the symmetric PCR amplification of the randomized single-stranded DNA library is overamplification. Overamplification is detrimental as it leads to the production of aberrant and spurious PCR products of different sizes, negatively affecting the entire SELEX experiment (Citartan et al. 2012). In a study conducted by Tolle and his colleagues, sequencing result of the nucleic acid pool from SELEX Cycle 8 revealed several other sequences of different lengths, made up of

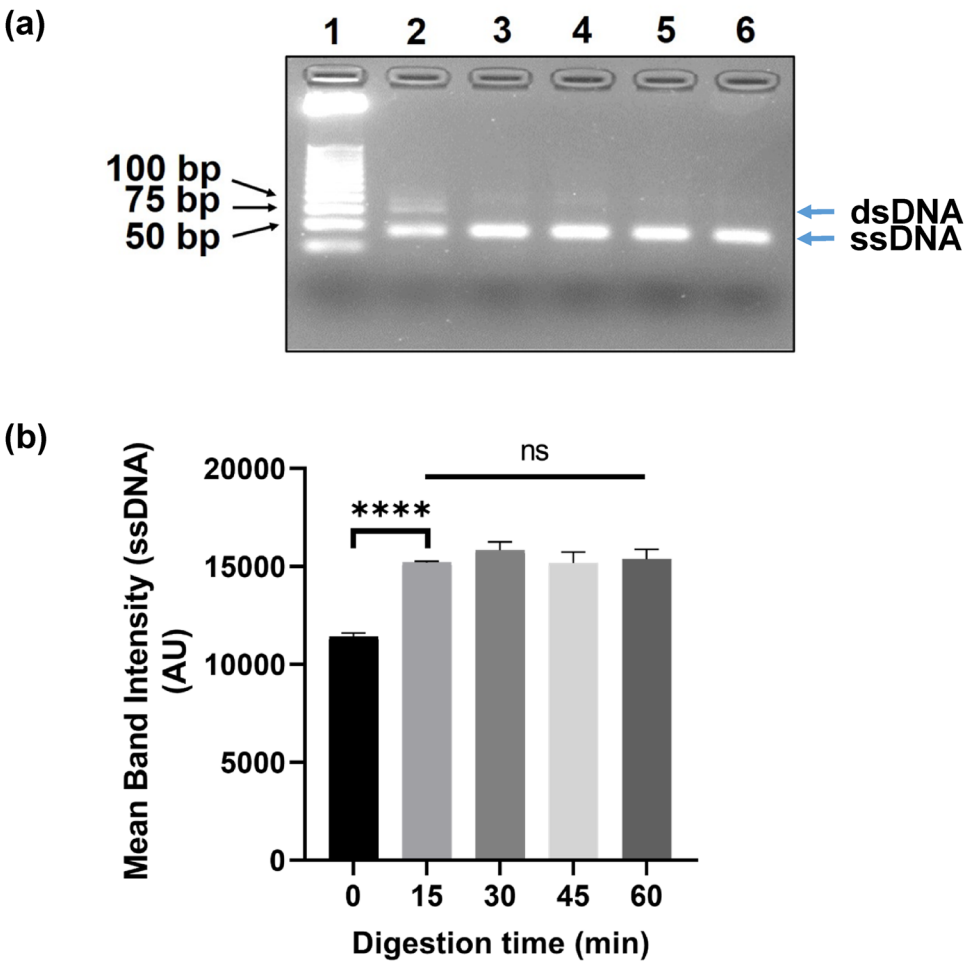

Fig. 6 Time course analysis of Lambda exonuclease digestion from 15 to 60 min. **a** 4% agarose gel electrophoresis of A-PCR products resulting from different lambda exonuclease digestion times. Lane 1: 25 bp DNA ladder, Lane 2: 15 min, Lane 3: 30 min, Lane 4: 45 min, Lane 5: 60 min **b** Bar graph of band intensities of ssDNA (A-PCR) produced from different lambda exonuclease digestion times as estimated by ImageJ analysis. Error bars represent standard deviation of 3 replicates. $P < 0.05$ was considered as statistically significant while ****$P < 0.0001$ and ns: not significant

concatenated multiple forward or reverse primer binding regions, without any enrichment of target binders (Tolle 2014). Hence, in this study, the effect of two main parameters, such as the amount of primer and the number of PCR cycles were optimized in the symmetric PCR amplification.

From our findings, extending the PCR cycles up to 6 cycles clearly resulted in the appearance of smeary bands. The intensity of the smeary band resulted from 6 PCR cycles is significantly higher than that of 5 PCR cycles. While there is no significant difference between the dsDNA band intensity between cycle 6 and cycle 5, we decided that 5 PCR cycles is enough to produce the dsDNA amplicon prior to the A-PCR amplification (Fig. 1a and b). Using higher number of PCR cycles could give way towards the appearance of higher molecular weight PCR product as the nature of the amplification of single-stranded DNA library, which consists of millions of sequences is different from that of the amplification of a single-target in a conventional PCR. The diversity of the sequences could complicate the amplification process as millions of different targets which vary in GC-content and the presence of a myriad of secondary structures assumed by these sequences could confound the nature of the amplification. Millions of sequences with different secondary structures could themselves also act as the template, causing the appearance of the higher molecular weight PCR product, which appear as smeary bands. Limiting the number of PCR cycles sufficient enough to produce dsDNA is the best strategy to minimize overamplification. Moreover, we have also optimized the amount of primer for the symmetric PCR and decided to choose an amount of 80 pmol, due to the highest dsDNA band intensity produced in comparison to the rest of the primer amounts (Fig. 2a and b). There is no significant difference in the dsDNA band intensity when 90 and 100 pmol primers were used. As such, the lowest amount, which is 80 pmol was determined as the amount of primer for an optimum production of dsDNA template.

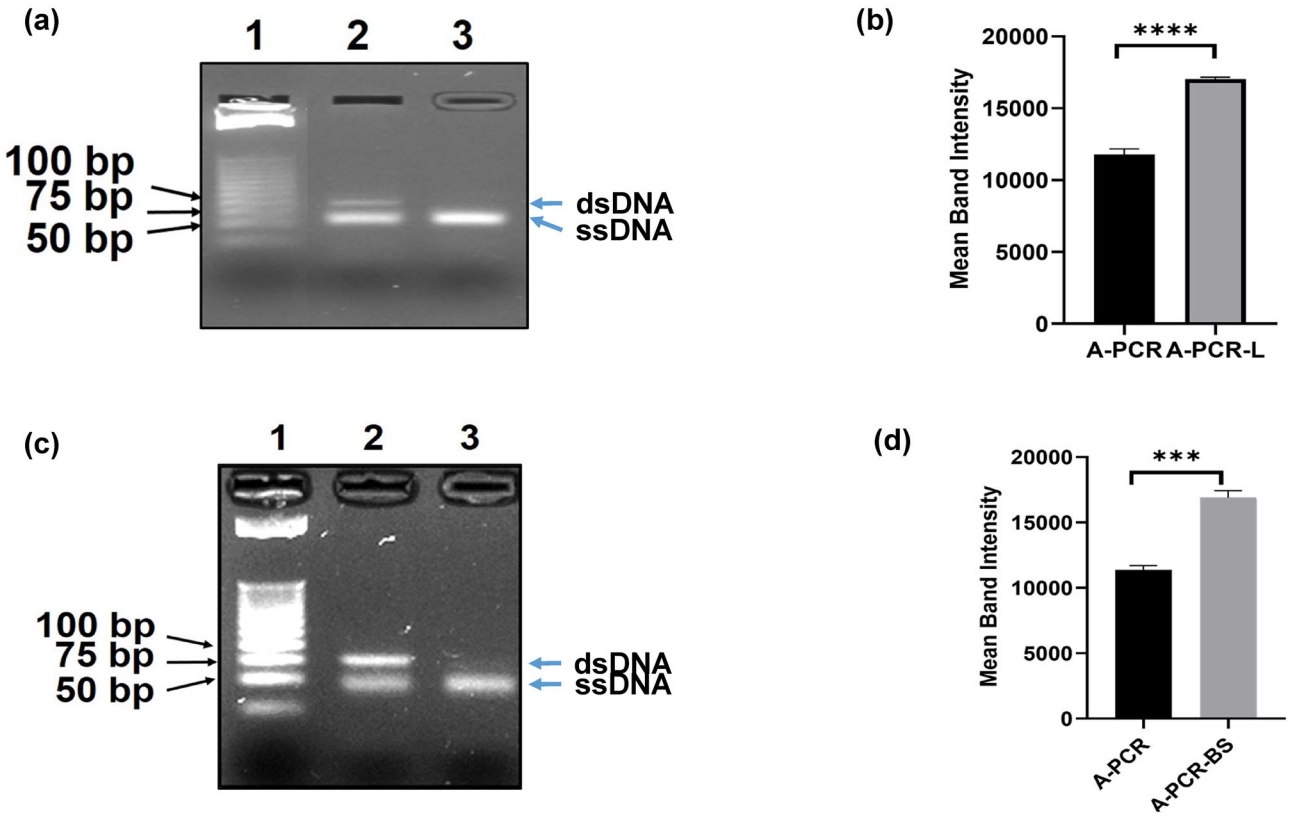

Fig. 7 Effects of the incorporation of Lambda exonuclease digestion and biotin-streptavidin separation into A-PCR on the ssDNA intensity. **a** 4% agarose gel electrophoresis of products produced from A-PCR and A-PCR-lambda exonuclease digestion. Lane 1: 25 bp DNA ladder, Lane 2: A-PCR and Lane 3: A-PCR-lambda exonuclease digestion. **b** Bar graph of band intensities of ssDNA produced from A-PCR and A-PCR-lambda exonuclease digestion as estimated by ImageJ analysis. Error bars represent standard deviation of 3 replicates. $P < 0.05$ was considered as statistically significant while $^{****}P < 0.0001$. **c** 4% agarose gel electrophoresis of products produced from A-PCR and A-PCR-biotin-streptavidin separation. Lane 1: 25 bp DNA ladder, Lane 2: A-PCR and Lane 3: A-PCR-biotin-streptavidin separation. **d** Bar graph of band intensities of ssDNA produced from A-PCR and A-PCR-biotin-streptavidin separation as estimated by ImageJ analysis. Error bars represent standard deviation of 3 replicates. $P < 0.05$ was considered as statistically significant while $^{***}P < 0.001$

Table 1 Yield of ssDNA generated by our method

ssDNA generation method	Amount of ssDNA recovered (nM)	Time (h)	Cost (USD)	Amount of ssDNA recovered by Svobodova et al. (nM)
A-PCR	450 ± 10.2	1	7	106 ± 39
A-PCR-lambda exonuclease	700 ± 11.3	1.5	8	274 ± 23.8
A-PCR-biotin-streptavidin	820 ± 19.2	1.5	14	–

Optimization of the A-PCR cycle

Using the purified dsDNA template, the next step in the optimization pipeline is finding the best parameters to ensure the optimum production of ssDNA in the A-PCR amplification. Parameters scrutinized in this study involves annealing temperatures, ratio of primers, concentrations of dsDNA template, number of PCR cycles, concentrations of dNTP/$MgCl_2$ and the amount of Taq DNA Polymerase.

The best annealing temperature chosen was 56.9 °C while 50:1 was determined as the best primer ratio

Our analysis of the annealing temperature revealed that 56.9 °C as the optimum temperature that could produce the best yield of ssDNA (Fig. 3a and b). Increasing the temperature beyond this value proved to be a futile effort as the yield of ssDNA dwindles. A high annealing temperature could debilitate the hybridization of the primers to the primer binding region, lowering the amplification

efficiency. As such, the yield of the ssDNA is poor when the annealing temperature increases. Our findings are also in line with the annealing temperature analysis performed by Heiat et al. (2017), who have also discovered that temperature range between 55 and 59 °C was the most suitable temperature for the amplification of ssDNA.

One of the most pivotal parameters to be optimized in an A-PCR amplification is the primer ratio. We have tested several different primer ratios such as 20:0, 20:0.5, 20:1, 20:2, 50:1 and 100:1. The ratio of 50:1 promoted the best amplification of ssDNA, which is significantly higher than the rest of the primer ratios except for 100:1 (Fig. 3a and b). We have chosen 50:1 as compared to 100:1 as less primers were consumed. Our result agreed with the findings by Heiat et al., 2017, who have also stated that 50:1 appeared to be the best primer ratio for the SELEX cycles from 2 cycles onward. As the second phase of the A-PCR amplification is of arithmetic nature, a primer ratio as high as 50:1 would be able to promote the amplification as more forward primers are available to synthesize new molecules of ssDNA.

The number of PCR cycles and the initial amount of dsDNA template play a prominent role in the A-PCR

The concentrations of DNA template were also subjected to optimization. Different concentrations of DNA template from 0.2, 0.4, 0.6 and 1.6 ng/uL of DNA template were used. From Fig. 4a and b, it is evidenced that the concentration of the DNA template of 1.6 ng/uL was the optimum value that could engender the highest ssDNA band intensity. The usage of more DNA template provides more starting material that would eventually thrive to give rise to ssDNA following exponential and arithmetic amplification.

Akin to symmetric PCR, the number of PCR cycles in an A-PCR reaction should also be optimized to maximize the yield of ssDNA while minimizing overamplification. In this study, the A-PCR was carried out using several different PCR cycles from 10 to 30 cycles. The best number of cycles was discovered to be 30, based on the highest ssDNA band intensity (Fig. 4c and d). In this study, despite increasing the PCR cycles up to 30, no smeary bands were produced. Our findings contradict the optimization result from other studies (Tabarzad et al. 2014; Heiat et al. 2017) and even our previous study, which strongly suggests the need for optimization of each individual library prior to the selection of the best parameters for A-PCR amplification.

Optimizing the concentrations and the amount of dNTP/$MgCl_2$ and Taq Polymerase, respectively resulted in no significant improvement in the amount of ssDNA

We have also investigated the effect of various concentrations of dNTP/$MgCl_2$ from 0.2 mM/1.5 mM, 0.4 mM/2.0 mM, 0.6 mM/2.5 mM, 0.8 mM/3.0 mM and 1.0 mM/3.5 mM on A-PCR. A standard dNTP/$MgCl_2$ concentration of 0.2 mM/1.5 mM was sufficient for an optimum amplification, based on the highest ssDNA band intensity (Figs. 5a and b). We have also investigated the effect of different amounts of Taq Polymerase on the ssDNA production of the A-PCR. No significant difference in the ssDNA band intensity was found when 2.5 units, 5 units and 10 units of Taq DNA polymerase were used (Fig. 5a and b). However, increasing the amount of Taq DNA polymerase caused the reduction in the band intensity of the ssDNA. We reckoned that the presence of too much of Taq Polymerase is inhibitory to the amplification reaction. A significant difference in the band intensity was observed when 2.5 units of Taq DNA polymerase was used as compared to 15 and 25 units of Taq DNA polymerase. A standard amount of Taq DNA polymerase, which is 2.5 units was found to be the best amount to ensure an optimal A-PCR amplification. In fact, the usage of Taq Polymerase can introduce mutations to the aptamers, which could potentially contribute to a better binding functionality against their cognate target (Schütze 2011).

Table 2 Comparison of the optimization of the parameters in the A-PCR

Parameters	This study	Citartan (2012)	Tabarzad et al. (2014)	Heiat et al. (2017)
PCR cycles	30	20	25	20
Primer ratio	50:1	20:1	15:1	50:1
Annealing temperature (°C)	56.9	–	64	59
Template concentration (ng/μL)	1.6	–	–	2
Mg^{2+}/dNTP concentration (mM)	0.2/1.5	–	0.25	–
Taq polymerase (U)	2.5 U	–	–	–

Comparison of the optimization in this study to that of the other studies performed-What have we learned

Optimization of the A-PCR in this study was compared with that of Citartan et al. (2012), Tabarzad et al. (2014) and Heiat et al. (2017). The optimized parameters were tabulated as can be seen in Table 2. Collectively, none of the studies including the present study overlap with each other in the values of the optimized A-PCR parameters, which implies the need to optimize for each different library prior to the start of any SELEX experiment. While all the libraries have different lengths, the sequence analysis between all the different libraries reveals no sequence similarity and as a consequence each library is expected to adopt a myriad of secondary structures that may vary tremendously from each other. The large differences in the pattern of secondary structures between each library may affect the amplification efficiency of the A-PCR to different degrees. Premising on this, overlapping values of the parameters across all these studies can never be expected, which corroborates the importance of optimizing the A-PCR amplification for each different library before embarking on any SELEX experiment to ensure an optimum yield of ssDNA from each SELEX cycle.

Incorporation of the ssDNA generation method further improves the yield of ssDNA of the A-PCR reaction

A-PCR amplification produces both ssDNA and dsDNA due to the biphasic amplification, which consists of both the logarithmic and linear amplification. The logarithmic phase of A-PCR accounts for the presence of dsDNA and we suppose that the remnant dsDNA can be converted to ssDNA to further improve the yield of the latter. In the present study, we have coupled A-PCR assay with another strategy of ssDNA generation. In the first strategy, we have utilized lambda exonuclease digestion, which is based on the enzyme known as lambda exonuclease that selectively excise phosphorylated strand of a dsDNA, leaving another strand in the form of ssDNA. The undigested strand, remaining as ssDNA combines with the existing ssDNA in the A-PCR reaction, increasing the total amount of ssDNA. Prior to the lambda exonuclease digestion assay, a time course analysis was performed from 15 to 60 min to find out the optimum digestion time without the issue of over-digestion of ssDNA. We discovered that 15 min of digestion is enough to remove the dsDNA, while extending the digestion time up to 60 min resulted in no significant difference in the dsDNA intensity (Fig. 6a and b). Having determined the time of digestion, we carried out an A-PCR reaction and subjected the reaction to the lambda exonuclease digestion. As can be observed from Fig. 7a and b, a dramatic increase in the ssDNA band intensity suggests that the incorporation of the lambda exonuclease digestion step can further increase the yield of ssDNA of the A-PCR reaction. Similar enhancement of the ssDNA band intensity can be seen from Fig. 7c and d, which also supports the potency of biotin-streptavidin-mediated separation in augmenting the yield of ssDNA.

A-PCR-biotin-streptavidin-mediated separation and A-PCR-lambda exonuclease digestion as the ideal methods for the generation of ssDNA

All the resulting A-PCR, A-PCR-lambda exonuclease and A-PCR-biotin-streptavidin-mediated separation reactions were subjected to purification. As a whole, compared to the yield reported by Svobodová et al. (2012), we have obtained a much higher yield of ssDNA following the purification of the A-PCR, A-PCR-lambda exonuclease digestion and A-PCR-biotin-streptavidin-mediated separation product (Table 2). The most possible reason for the higher yield is the much extensive optimization of the A-PCR reactions, which have bolstered the yield of ssDNA prior to the additional ssDNA purification.

Similar to the results from Svobodova's group, our findings show that the incorporation of ssDNA step such as lambda exonuclease digestion (700 ± 11.3 nM) and biotin-streptavidin separation (820 ± 19.2 nM) significantly improved the yield of ssDNA as compared to A-PCR alone (450 ± 10.2 nM). As an ideal ssDNA-generating techniques, both the A-PCR-lambda exonuclease digestion and A-PCR-biotin-streptavidin separation are able to generate a high amount of ssDNA at an affordable cost. A high amount of ssDNA generated is able to minimize the chance of losing potential binders of a SELEX experiment during the purification of ssDNA. Compared to A-PCR, the A-PCR-lambda exonuclease digestion appears to be more prominent due to its ability to generate the amount of ssDNA approximately twofold higher than that of A-PCR alone. This can be achieved at a similar cost albeit with a slightly longer duration. Compared to the A-PCR-lambda exonuclease digestion, A-PCR-biotin-streptavidin seems to be able to produce a higher yield of ssDNA. However, in terms of cost, A-PCR-lambda exonuclease digestion is preferred over A-PCR-biotin-streptavidin due to the much lower cost. However, in terms of time, both these techniques require similar duration. The most prominent finding from our study is the significance of developing an optimization pipeline for the A-PCR reaction prior to the purification and additional ssDNA generation strategy, which could augment the yield of ssDNA.

Conclusion

We have successfully developed an optimization pipeline of the A-PCR reaction, demonstrating the step-by-step optimization of the parameters that could improve the yield of the ssDNA. An additional ssDNA generation step was also included in the pipeline to further augment the yield of ssDNA. We have successfully obtained a value of up to 700 ± 11.3 and 820 ± 19.2 nM using two different additional ssDNA generation strategy. It is strongly recommended to develop a separate optimization pipeline of A-PCR for each different randomized ssDNA library before initiating any SELEX experiment.

Acknowledgements We acknowledge the Ministry of Higher Education, Malaysia for Skim Latihan Akademik Bumiputra (SLAB). We declare no conflict of interest in regards to this manuscript.

Funding Citartan M and Tang TH were supported by USM Research University Grant (1001.CIPPT.8011095).

References

Avci-Adali M et al (2009) Upgrading SELEX technology by using lambda exonuclease digestion for single-stranded DNA generation. Molecules (basel) 15(1):1–11

Bilibana MP et al (2017) Aptamers as the agent in decontamination assays (Apta-Decontamination Assays): from the environment to the potential application in vivo. J Nucleic Acids 2017:3712070

Citartan M et al (2011) Conditions optimized for the preparation of single-stranded DNA (ssDNA) employing lambda exonuclease digestion in generating DNA aptamer. World J Microbiol Biotechnol 27(5):1167–1173

Citartan M et al (2012) Asymmetric PCR for good quality ssDNA generation towards DNA aptamer production. Songklanakarin J Sci Technol 34:125–131

Citartan M et al (2016) Aptamers as the 'capturing' agents in aptamer-based capture assays. Microchem J 128:187–197

Citartan M et al (2019) Aptamers as the chaperones (Aptachaperones) of drugs-from siRNAs to DNA nanorobots. Int J Pharm 567:118483

Citartan M (2021) The dynamicity of light-up aptamers in one-pot in vitro diagnostic assays. Analyst

Ellington AD, Szostak JW (1990) In vitro selection of RNA molecules that bind specific ligands. Nature 346(6287):818–822

Elskens JP, Elskens JM, Madder A (2020) Chemical modification of aptamers for increased binding affinity in diagnostic applications: current status and future prospects. INt J Mol Sci 21(12):127

Hao M, Qiao J, Qi H (2020) Current and emerging methods for the synthesis of single-stranded DNA. Genes (basel). 11(2):116

Heiat M et al (2017) Essential strategies to optimize asymmetric PCR conditions as a reliable method to generate large amount of ssDNA aptamers. Biotechnol Appl Biochem 64(4):541–548

Hermann T, Patel DJ (2000) Adaptive recognition by nucleic acid aptamers. Science 287(5454):820–825

Li L et al (2021) Nucleic acid aptamers for molecular diagnostics and therapeutics: advances and perspectives. Angew Chem Int Ed Engl 60(5):2221–2231

Liu LS et al (2021) Recent developments in aptasensors for diagnostic applications. ACS Appl Mater Interfaces 13(8):9329–9358

McKeague M, DeRosa MC (2012) Challenges and opportunities for small molecule aptamer development. J Nucleic Acids 2020:748913

Mosing RK, Bowser MT (2009) Isolating aptamers using capillary electrophoresis–SELEX (CE–SELEX). In: Mayer G (ed) Nucleic acid and peptide aptamers: methods and protocols. Humana Press, Totowa, pp 33–43

Nomura Y et al (2010) Conformational plasticity of RNA for target recognition as revealed by the 2.15: a crystal structure of a human IgG-aptamer complex. Nucleic Acids Res 38(21):7822–7829

Odeh F et al (2019) Aptamers chemistry: chemical modifications and conjugation strategies. Molecules 25(1):3

Piganeau N, Schroeder R (2003) Aptamer structures: a preview into regulatory pathways? Chem Biol 10(2):103–104

Schütze T et al (2011) Probing the SELEX process with next-generation sequencing. PLoS ONE 6(12):29604

Svobodová M et al (2012) Comparison of different methods for generation of single-stranded DNA for SELEX processes. Anal Bioanal Chem 404(3):835–842

Tabarzad M et al (2014) Challenges to design and develop of DNA aptamers for protein targets. I. Optimization of asymmetric PCR for generation of a single stranded DNA library. Iran J Pharm Res 13:133–141

Thevendran R et al (2020) Strategies to bioengineer aptamer-driven nanovehicles as exceptional molecular tools for targeted therapeutics: a review. J Control Release 323:530–548

Tolle F et al (2014) By-product formation in repetitive PCR amplification of DNA libraries during SELEX. PLoS ONE 9(12):114693

Tuerk C, Gold L (1990) Systematic evolution of ligands by exponential enrichment: RNA ligands to bacteriophage T4 DNA polymerase. Science 249(4968):505–510

Wang J et al (2021) Development of aptamer-based molecular tools for rapid intraoperative diagnosis and in vivo imaging of serous ovarian cancer. ACS Appl Mater Interfaces 13(14):16118–16126

Authors and Affiliations

Tzi Shien Yeoh[1] · Andrew Anna[1,2] · Thean-Hock Tang[1] · Marimuthu Citartan[1]

✉ Marimuthu Citartan
citartan@usm.my

[1] Advanced Medical & Dental Institute (AMDI), Universiti Sains Malaysia, 13200 Bertam, Kepala Batas, Penang, Malaysia

[2] Faculty of Medicine and Health Sciences, Universiti Malaysia Sarawak (UNIMAS), 93400 Kota Samarahan, Sarawak, Malaysia